Journal of Thermal Analysis, Vol. 30 (1985) 399–427

THERMAL DECOMPOSITION OF HALO-BIS(PIPERIDYLDITHIO-CARBAMATES) OF As(III), Sb(III) AND Bi(III)
Estimation of kinetic parameters (k, n) of some dithiocarbamates by QIA techniques

M. Lalia-Kantouri, A. Christofides* and *G. E. Manoussakis*

DEPARTMENT OF GENERAL AND INORGANIC CHEMISTRY, THESSALONIKI, GREECE

(Received September 3, 1984)

Simultaneous TG/DTG/DTA studies under non-isothermal conditions have been carried out in air and nitrogen on some halo-dithiocarbamates of the general formula $XM[S_2CN(CH_2)_5]_2$ (X = Cl, Br and I; and M = As, Sb and Bi). E^* values for the 1st stage of decomposition were determined by graphical methods and the TTN temperatures were calculated from the TG profiles. A possible mechanism of the decomposition reaction is suggested, based on the thermoanalytical and pyrolysis results and the mass spectral data.

The kinetic analysis data on five of the above dithiocarbamates and nine complexes of the general formula $M[S_2CN<]_3$ (M = As, Sb and Bi; and $N< = NEt_2$, $N(CH_2)_5$ and $N(CH_2)_4O$) were studied by the QIA (quasi-isothermal analysis) technique in air atmosphere. An example of kinetic parameter (k and n) estimation for the first decomposition stage is given for $Bi[S_2CN(CH_2)_5]_3$, with the assumption of different kinetic equations.

A literature survey reveals that little work has been done on the thermal decomposition of halo-dithiocarbamate complexes [1–5], and the reports are mainly confined to tin complexes [1–4]. The first published papers deal with the pyrolysis of dihalotin(IV) bis(diethyldithiocarbamate) in an inert atmosphere to yield carbon disulphide and tetraethylthiourea as the major products. The main intermediates in the solid phase are $Cl_2Sn(NCS)_2$ [1] or X_2SnS (X = Cl, Br and I) [2, 3], which subsequently decompose to give tin sulphide. Recently, Kaushik et al. [4] reported the thermal investigation of $Sn(PED)_2Cl_2$ (PED = *p*-ethoxyphenyldithiocarbamate), which led to the same results.

Continuing our previous work on metal dithiocarbamates [6, 7], in the present paper we describe the thermal investigation (TG/DTG/DTA, pyrolysis and MS) of halo-bis(piperidyldithiocarbamates) of As(III), Sb(III) and Bi(III) of the general type $XM[S_2CN(CH_2)_5]_2$ (X = Cl, Br and I; and M = As, Sb and Bi).

* Author to whom correspondence should be addressed.

John Wiley & Sons, Limited, Chichester
Akadémiai Kiadó, Budapest

The thermal decomposition kinetics of fourteen dithiocarbamates of As(III), Sb(III) and Bi(III) have also been studied in this paper by means of the QIA (quasi-isothermal analysis) technique in air atmosphere.

The kinetic analysis of TG data obtained under non-isothermal conditions does not allow the determination of whether a solid decomposition reaction is of n order or follows the Prout–Tompkins, the Avrami–Erofeev or a diffusion mechanism. However, the equations developed for the kinetic analysis of TG curves obtained with the QIA technique permit differentiation of the above mechanisms.

Quasi-isothermal analysis (QIA), which was first developed by J. and F. Paulik [8, 9], is a very useful thermogravimetric technique. This method programs the reaction temperature in such a way that the decomposition rate of the sample is kept constant at an arbitrarily selected particular value. Compared to non-isothermal thermogravimetry, close-lying reactions can be separated easily and kinetic data can be obtained for each intermediate reaction in a single run. Rouquerol [10] has described the kinetic analysis of TG curves of n order reactions by this procedure.

Kinetics: Theoretical

The shapes of the weight and temperature curves taken under QIA conditions can be informative concerning the mechanism controlling the reaction [11, 12]. Once the extent of the individual intermediate reactions is established, the fraction of the reactant decomposed (a) can easily be calculated ($a = W_t/W_{max}$, where W_t is the weight loss at a certain time t, and W_{max} is the weight loss at the end of transformation).

The general expression for the reaction rate of a heterogeneous reaction is

$$\frac{da}{dt} = Ae^{-\frac{E}{RT}} \cdot f(a) \tag{1}$$

where $f(a)$ is a function depending on the reaction mechanism. For n order reactions, $f(a) = (1-a)^n$. By integrating Eq. (1) and making the substitution

$$g(a) = \int_0^a \frac{da}{f(a)} \tag{2}$$

Eq. (1) becomes

$$g(a) = kt \tag{3}$$

where k is the rate constant of the decomposition reaction.

The algebraic expressions of the function $f(a)$ and $g(a)$ corresponding to the mechanisms commonly used in the literature for the thermal decomposition of solids have been summarized in papers [13, 14].

Experimental

All complexes were prepared by known methods [15–17]; they were recrystallized from a mixture of CH_2Cl_2–C_2H_5OH, and dried under vacuum. The thermal decomposition was carried out on a Netsch 429 equipment at a heating rate of 2 deg/min, in the temperature region 20–600°, using a sample mass of 25 mg and α-Al_2O_3 as reference. The measurements under non-isothermal conditions were performed in a dynamic atmosphere of air or nitrogen.

Pyrolysis of the iodo-bis(piperidyldithiocarbamates) was carried out in a dynamic nitrogen atmosphere, using the technique applied in our earlier work [6].

QIA measurements in air were made with a Netsch 429 equipment, which is equally suitable for simultaneous TG/DTG/DTA examinations under dynamic heating conditions and quasi-isothermal TG/DTG measurements. The heating rate was 5 deg/min and the sample mass, in a covered crucible, was around 25 mg. The rate of transformation was selected to be 0.2 mg/min.

X-ray powder diffraction analyses of the final residues were made with a Phillips PW 11300/00 X-ray diffractometer, using Cu–Ka radiation. For the determination of TTN, the areas of the TG curves were measured with a Coradi Cora-Senior planimeter. Carbon, hydrogen and nitrogen determinations were performed on a Perkin–Elmer microanalyser. Infrared spectra were recorded in the range 4000–250 cm^{-1} on a Perkin–Elmer 467 spectrophotometer, using KBr pellets. Mass spectra were recorded on an R. M. V.-6L-Hitachi–Perkin–Elmer mass spectrometer.

Results and discussion

Thermal analysis

The thermoanalytical curves (TG/DTG and DTA) of halo-bis(piperidyldithiocarbamate) complexes, under non-isothermal conditions, in dynamic atmospheres of air and nitrogen, are given in Figs 1 to 10. In all cases the decomposition process over the temperature range from 20 to 600° includes various thermal effects. From the TG and DTA profiles, it is obvious that the first and main decomposition stage displays similarities in air and nitrogen, and for the iodo derivatives begins without melting.

The following stages are also quite similar, but differ as to the temperature ranges in which they occur. In nitrogen, all the decomposition reactions are endothermic, whereas in air the majority of them are exothermic, demonstrating the oxidative effect of oxygen on the studied complexes.

The final residues of all the studied halo-dithiocarbamate complexes in a nitrogen atmosphere are elemental metals (M^0) or metal sulphides (MS), the latter being produced from a mixture of $M + M_2S_3$, where the metal appears to be in greater proportion. For the corresponding tris(dithiocarbamates), however, the final residues contain only M_2S_3 [6, 7]. In air, the solid residues are Sb_2O_4 and $(BiO)_2SO_4$, whereas

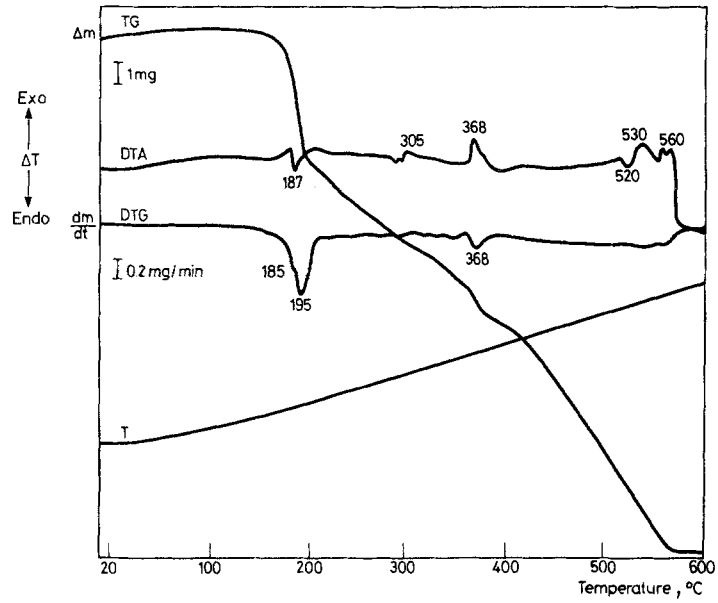

Fig. 1 Thermoanalytical curves for $IAs[S_2CN(CH_2)_5]_2$ in air

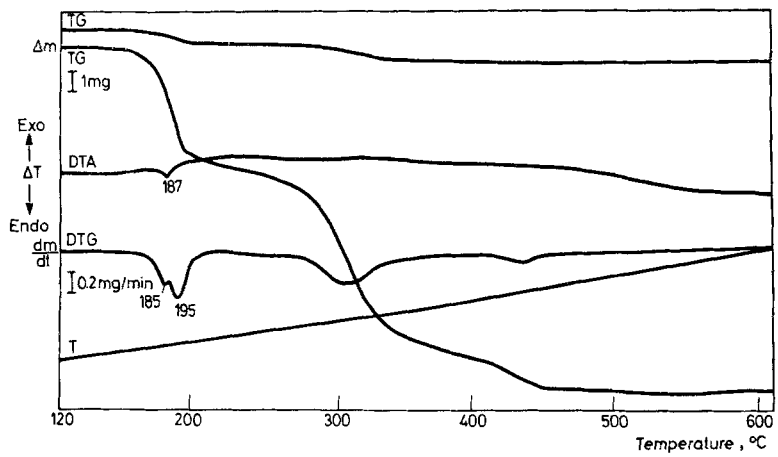

Fig. 2 Thermoanalytical curves for $IAs[S_2CN(CH_2)_5]_2$ in nitrogen

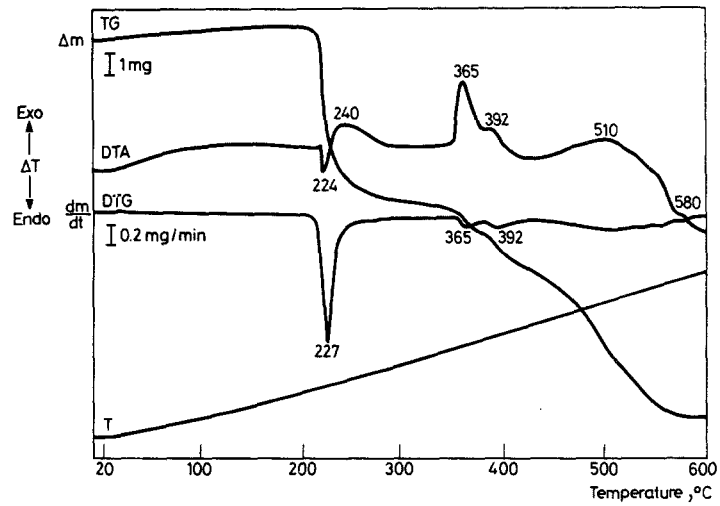

Fig. 3 Thermoanalytical curves for $ISb[S_2CN(CH_2)_5]_2$ in air

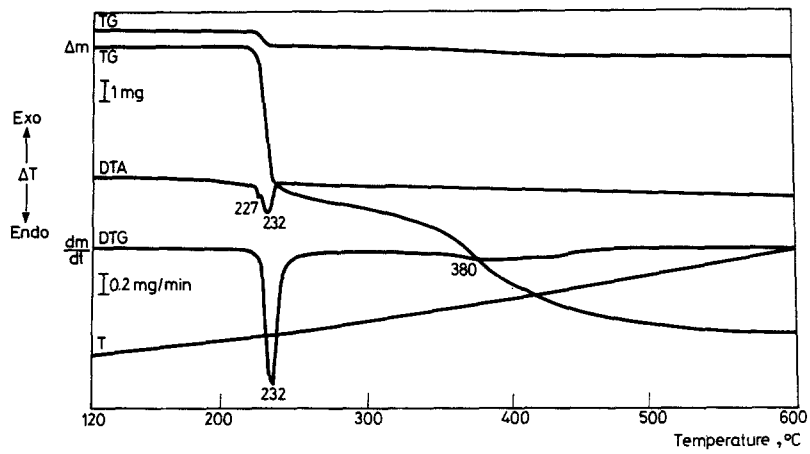

Fig. 4 Thermoanalytical curves for $ISb[S_2CN(CH_2)_5]_2$ in nitrogen

the As analogues leave the crucible completely empty, due to the volatility of the As_4O_6 formed, as in the case of the tris(piperidyldithiocarbamates) of the same metals [6].

The temperature ranges and percentage mass losses of the various decomposition stages are given in Tables 1 to 4. The temperatures of the greatest rate of decomposition (DTG_{max}), the theoretical percentage mass losses, and the DTA data are also given.

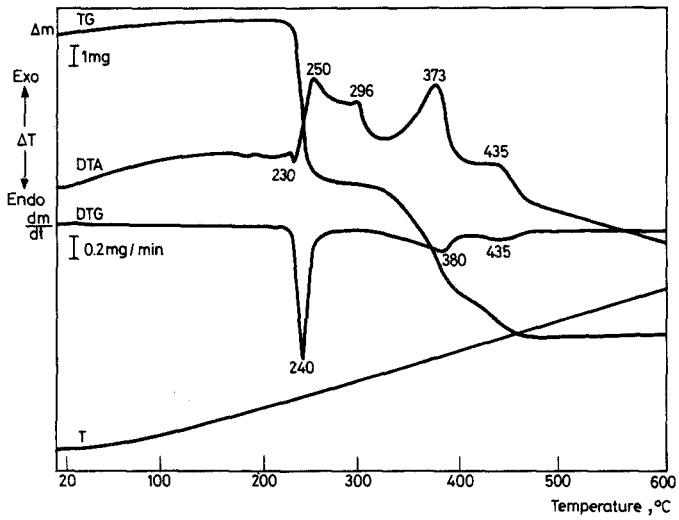

Fig. 5 Thermoanalytical curves for $IBi[S_2CN(CH_2)_5]_2$ in air

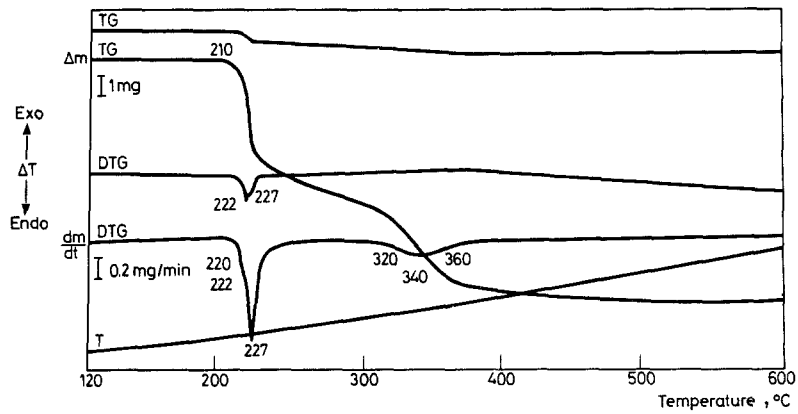

Fig. 6 Thermoanalytical curves for $IBi[S_2CN(CH_2)_5]_2$ in nitrogen

The thermoanalytical data obtained on the iodo derivatives show that in the first decomposition stage a iodine atom is evolved initially, followed by rupture of the M–S bond only in the As(III) and Bi(III) complexes, which results in the removal of one dithiocarbamato group or one carbon disulphide. In the bismuth complex, a iodine atom and one molecule of CS_2 are evolved simultaneously. Thus, we can conclude that the metal-sulphur bond is thermally more stable in the arsenic complex than in the complexes of antimony and bismuth. Further support for this conclusion

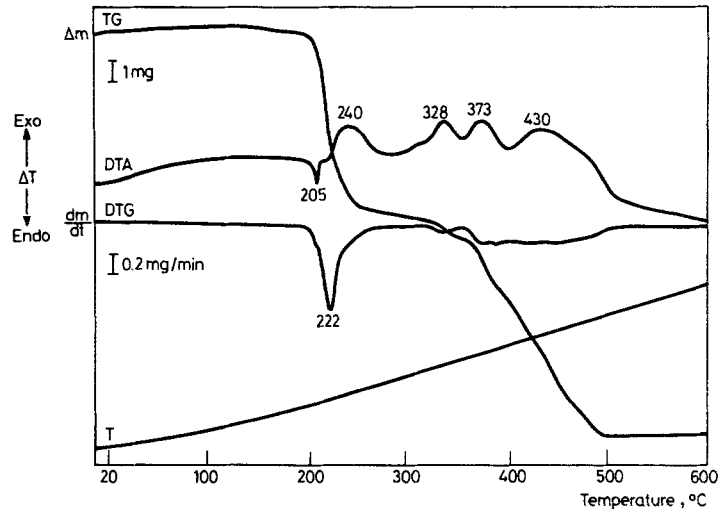

Fig. 7 Thermoanalytical curves for $BrSb[S_2CN(CH_2)_5]_2$ in air

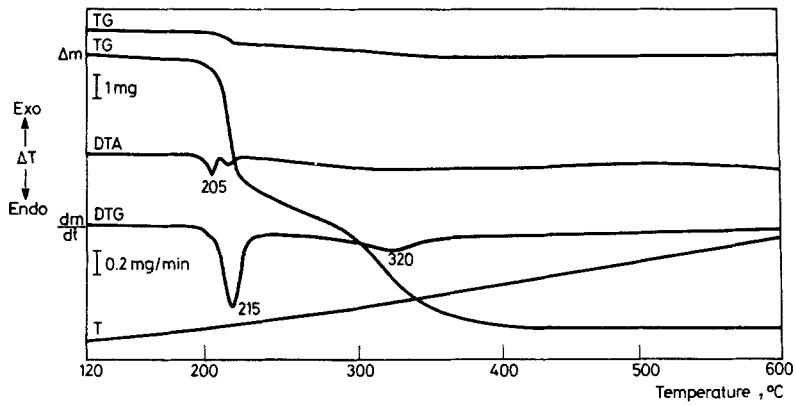

Fig. 8 Thermoanalytical curves for $BrSb[S_2CN(CH_2)_5]_2$ in nitrogen

is provided by the crystallographic data on the complexes $M[S_2CNEt_2]_3$ (M = As, Sb and Bi) [18, 19], which show that the length of the M–S bond increases on going from arsenic to bismuth. This lengthening decreases the strength of the bond, resulting finally in its easier rupture.

From the thermoanalytical data obtained on the complexes $XSb[S_2CN(CH_2)_5]_2$ (X = Cl, Br and I), it is evident that they lose a chlorine plus one dithiocarbamato group, or a bromine plus one molecule of carbon disulphide. The decreasing strength

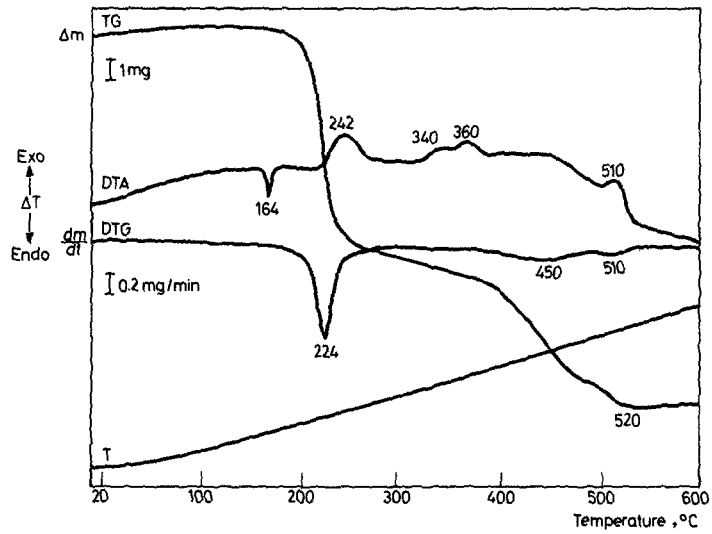

Fig. 9 Thermoanalytical curves for $ClSb[S_2CN(CH_2)_5]_2$ in air

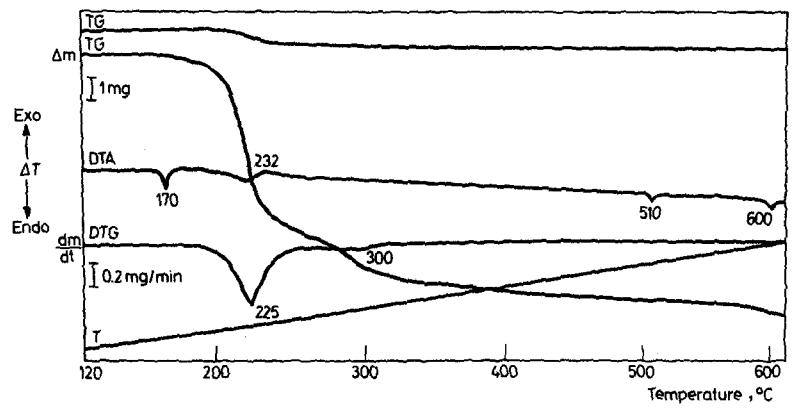

Fig. 10 Thermoanalytical curves for $ClSb[S_2CN(CH_2)_5]_2$ in nitrogen

of the Sb–S bond on going from iodo to chloro derivatives can be explained in terms of the back-donation effect from metal to sulphur, this being less for the chloro derivative, with overall weakening of the Sb–S bond.

The thermoanalytical curves for $BrSb[S_2CN(CH_2)_5]_2$ (Fig. 11), obtained in vacuum, indicate similarities with those in a nitrogen atmosphere. The thermoanalytical data are given in Table 4. The experimentally found percentage of the final residue (10.5%) is much lower than the calculated one (23.30%) if it is considered to

Table 1 Thermoanalytical results (TG/DTG/DTA) of iodo-bis(piperidyldithiocarbamates) of As(III), Sb(III), Bi(III) in air atmosphere

Complex	DTA results m.p., °C endothermic peak	DTA results Temperature peak, °C endothermic (–) exothermic (+)	Stage	TG/DTG results Temperature range, °C	TG/DTG results DTG_{max}, °C	Mass loss %	Evolved moiety Formula	Evolved moiety Mass calcd., %
$IAs[S_2CN(CH_2)_5]_2$	–	185 (+), 187 (–)	1	150–210	185, 195	24.1	I	24.32
				+			+	
		210 (+)		210–360		24.7	$SCN(CH_2)_5$	24.52
		368 (+)	2	360–400	368	6.5	S	6.13
		510 (+), 520 (–), 532 (+), 550 (–), 555 (+), 560 (+)	3	400–560	–	43.7	$SCN(CH_2)_5$ + As_2S_3	43.48
			residue	> 560		0	–	0
$ISb[S_2CN(CH_2)_5]_2$	–	224 (–), 240 (+)	1	215–227	227	21.6	I	22.30
				+			+	
				227–360		12.6	CS_2	13.35
		365 (+), 392 (+)	2 + 3	360–420–580	365, 392	36.5	$N(CH_2)_5 + SCN(CH_2)_5$	36.25
		510 (+)	residue	> 580		27.2	Sb_2O_4	27.04
$IBi[S_2CN(CH_2)_5]_2$	–	230 (–), 250 (+), 292 (+)	1	220–250	240	30.1	$I + CS_2$	30.89
		373 (+)	2	300–385	380	18.9	$SCN(CH_2)_5$	19.45
		435 (+)	3	385–460	435	10.0	$N(CH_2)_5$	12.78
			residue	> 460		41.0	$(BiO)_2SO_4$	41.58

Table 2 Thermoanalytical results (TG/DTG/DTA) of iodo-bis(piperidyldithiocarbamates) of As(III), Sb(III), Bi(III) in nitrogen atmosphere

Complex	DTA results		TG/DTG results			Mass loss, %	Evolved moiety	
	m.p., °C endothermic peak	Temperature peak, °C endothermic	Stage	Temperature range, °C	DTG_{max}, °C		Formula	Mass calcd. %
$IAs[S_2CN(CH_2)_5]_2$	–	187	1	150–220	185, 195	30.6	$S_2CN(CH_2)_5$	30.95
				or		or	or	or
				150–280		39.0	$I + CS_2$	39.25
			2	260–360	310	47.2	$I + SCN(CH_2)_5$	48.8
				or		or	or	or
				280–360		40.8	$N(CH_2)_5 + SCN(CH_2)_5$	40.6
			3	360–480	440	13.6	–	–
			residue	> 600		8.6	As	14.5
$ISb[S_2CN(CH_2)_5]_2$	–	233	1	220–260	233	35.0	$I + CS_2$	35.64
				+			+	
				260–300		15.6	$N(CH_2)_5$	14.95
			2	360–490	380	22.0	$SCN(CH_2)_5$	22.49
			residue	> 600		22.0	Sb	21.40
$IBi[S_2CN(CH_2)_5]_2$	–	222,227	1	215–250	222, 227	31.0	$I + CS_2$	30.89
				+			+	
				250–320		12.4	$N(CH_2)_5$	12.78
			2	320–360	340	15.8	$CN(CH_2)_5$	14.60
			residue	> 540		35.0	$Bi_2S_2(Bi_2S_3 + Bi^0)$	36.68

Table 3 Thermoanalytical results (TG/DTG/DTA) of halo-bis(piperidyldithiocarbamates) of Sb(III) in air atmosphere

Complex	DTA results m.p., °C endothermic peak	DTA results Temperature peak, °C endothermic (–) exothermic (+)	Stage	TG/DTG results Temperature range, °C	TG/DTG results DTG_{max}, °C	Mass loss, %	Evolved moiety Formula	Evolved moiety Mass calcd. %
$BrSb[S_2CN(CH_2)_5]_2$	205	218 (–), 240 (+)	1	190–250	222	32.30	$Br + CS_2$	29.90
							or	or
							$S_2C + N(CH_2)_5$	30.65
		335 (+)	2	320–370	335	5.84	S	6.13
		~ 430 (+)	3	370–500	375	34.00	$N(CH_2)_5 + CN(CH_2)_5$	34.48
							or	or
							$Br + CN(CH_2)_5$	34.20
			residue	> 500		23.30	Sb_2O_4	29.50
$ClSb[S_2CN(CH_2)_5]_2$	164	242 (+)	1	160–260	224	41.2	$Cl + S_2CN(CH_2)_5$	40.97
		340 (+), 360 (+)	2	260–370		6.3	S	6.70
				+			+	
		450 (+)		370–480	450	19.0	$CN(CH_2)_5$	20.08
		510 (+)	3	480–520	510	5.5	$Sb_2S_3 \rightarrow Sb_2O_4$	6.69
			residue	> 520		28.0	Sb_2O_4	32.00

Table 4 Thermoanalytical results (TG/DTG/DTA) of halo-bis(piperidyldithiocarbamates) of Sb(III)

Complex	DTA results		TG/DTG results			Mass loss, %	Evolved moiety	
	m.p., °C endothermic peak	Temperature peak, °C endothermic	Stage	Temperature range, °C	DTG_{max}, °C		Formula	Mass calcd., %
$ClSb[S_2CN(CH_2)_5]_2$	170	225	1	160–235	225	41.57	$S_2CN(CH_2)_5 + Cl$	40.97
			2	235–320	300	20.03	$CN(CH_2)_5$	20.08
(nitrogen)	510			320–560		7.4	S	6.70
	600		residue	> 560		31.0	$SbS(Sb_2S_3 + Sb^0)$	32.20
$BrSb[S_2CN(CH_2)_5]_2$	205	215	1	186–217	215	31.0	$S_2CN(CH_2)_5$	30.65
				+			+	
				217–280		15.0	Br	15.32
(nitrogen)			2	280–370	320	24.5	$SCN(CH_2)_5$	24.50
				370–500		5.5	S	6.13
			residue	> 500		24.0	Sb	23.30
$BrSb[S_2CN(CH_2)_5]_2$	200	215	1	180–217	215	32.75	$S_2CN(CH_2)_5$	30.65
				+			+	
				217–260	240	29.75	$Br + CS_2$	29.90
(vacuum 10^{-2} Torr)			2	460–560	520	20.0	$N(CH_2)_5$ + Sb partially	16.09
			residue	> 560		10.5	Sb partially	23.30

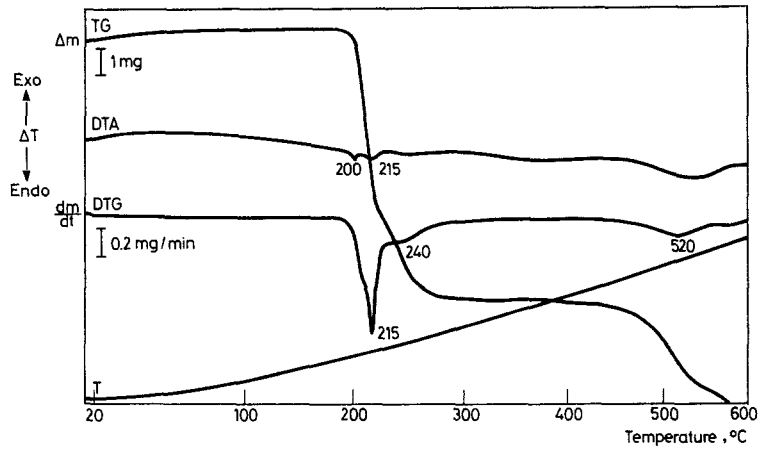

Fig. 11 Thermoanalytical curves for $BrSb[S_2CN(CH_2)_5]_2$ under vacuum

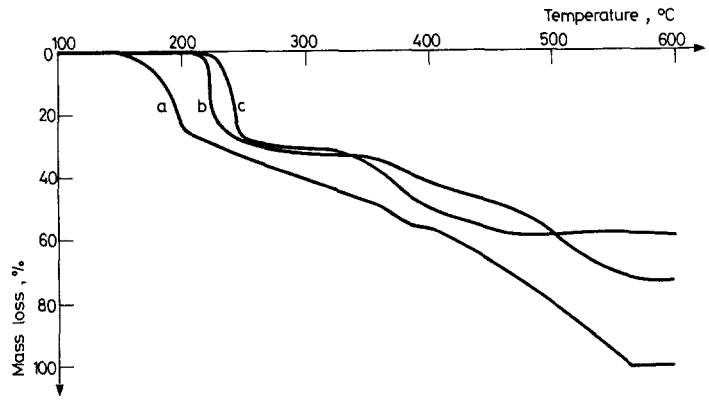

Fig. 12 Corrected TG curves of iodo-bis(piperidyldithiocarbamates) of As(III) (a), Sb(III) (b) and Bi(III) (c) in air

be elemental antimony. Unfortunately, the X-ray powder diffraction data are not sufficiently clear to elucidate its chemical nature.

Conclusively, we can say that our results show the dependence of the whole procedure of thermal decomposition of the studied complexes on the nature of the metal and on the nature of the halogen. This was established by determining the TTN [20] of the complexes from their corrected TG curves in air (Figs 12, 13), also taking into account the buoyancy effect. Thus, the TTN values (Table 5) for the complexes with the same ligands but different metals ($IM[S_2CN(CH_2)_5]_2$, Fig. 12) indicated that the decomposition temperature increases from the As to the Bi complex. For the complexes with the same ligands and the same metals, but different halogens ($XSb[S_2CN(CH_2)_5]_2$, Fig. 13), the TTN values indicated that the thermal stability

of these complexes follows the sequence Cl < Br < I. This is in accord with the strength and the length of the Sb–X bond [21] and with the electronegativities of the halogens.

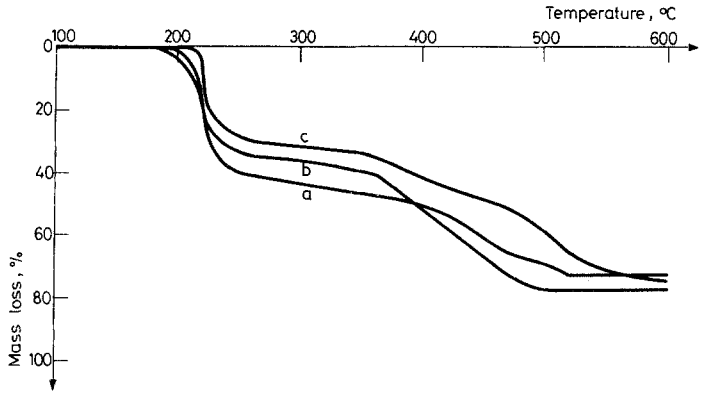

Fig. 13 Corrected TG curves of halo-bis(piperidyldithiocarbamates) of Sb(III) in air. (a) X = Cl, (b) X = Br, (c) X = I

Apparent activation energy (E^*)

E^* was calculated for the first decomposition stage for the complexes $IAs[S_2CN(CH_2)_5]_2$, $BrSb[S_2CN(CH_2)_5]_2$ and $ClSb[S_2CN(CH_2)_5]_2$ in air by the modified $n = 1$ method of Freeman–Carroll [22] and Piloyan's two methods [23]. The same methods applied to the iodo-bis(piperidyldithiocarbamate) complexes of Sb(III) and Bi(III) do not give acceptable E^* values.

The E^* values (Table 5) do not correlate well with the nature either of the metal or of the halogen, and consequently we have been unable to make comparisons. Furthermore, each of the three calculation methods employed gives values which differ significantly for a certain complex.

Table 5 Activation energy's values, E^*, and TTN temperatures of halo-bis(piperidyldithiocarbamates)

Complex	TTN, °C	Activation energy, E^*, kJ/mol		
		Freeman–Carroll ($n = 1$)	Piloyan TG	Piloyan DTG
$IAs[S_2CN(CH_2)_5]_2$	140	255	111	192
$ISb[S_2CN(CH_2)_5]_2$	213	–	–	–
$IBi[S_2CN(CH_2)_5]_2$	215	–	–	–
$BrSb[S_2CN(CH_2)_5]_2$	180	318	211	249
$ClSb[S_2CN(CH_2)_5]_2$	168	230	119	167

Pyrolysis and mechanism

A sample of the complex $ISb[S_2CN(CH_2)_5]_2$ was heated in nitrogen up to the end of the first and main decomposition stage. The compound appears first to shrink and the decomposition begins slowly. CS_2 was detected from its characteristic smell in a liquid-air trap. The salt $(CH_2)_5NCS_2^-H_2\overset{+}{N}(CH_2)_5$ and the sulphenamide $(CH_2)_5NC(=S)SN(CH_2)_5$ were found in small amounts.

A major decomposition product, isolated from the walls of the pyrolysis flask, was an orange solid compound. This solid, which melts at high temperature ($> 250°$), turned out to be an inorganic compound, since its ir spectrum shows no absorptions due to organic moieties. Moreover, the presence of iodine anions was detected. The black residue which remains after heating of the sample up to 250° contains mainly Sb_2S_3 and 20% carbon. Accordingly, we can say that the thermal decomposition of the iodo derivative appears to be similar to that of the corresponding tris(dithiocarbamate) complex.

By combining the thermogravimetric and the pyrolysis results on the above complex, as well as the similarities of its pyrolysis products with those of the tris(piperidyldithiocarbamate) complexes, we propose the following reaction path for the complex $IAs[S_2CN(CH_2)_5]_2$:

$$IAs[S_2CN(CH_2)_5]_2 \xrightarrow{-I^-,\ -\overset{+}{C}(=S)-N(CH_2)_5} SAs[S_2C\underline{N}(CH_2)_5]$$

In this path, the first and main decomposition step involves the homolytic dissociation of the arsenic–iodine bond and the subsequent removal of one piperidyldithiocarbamoylo group, and the presumed intermediate product $SAs[S_2CN(CH_2)_5]$ is formed. As the temperature is raised, this further decomposes to the possible products As and $(AsS)_2$, with concomitant loss of one dithiocarbamato group, from which the salt $(CH_2)_5NCS_2^-H_2\overset{+}{N}(CH_2)_5$, found amongst the pyrolysis products of the complexes can be formed.

As far as the corresponding complexes of Sb(III) and Bi(III) are concerned, in the former homolytic dissociation of the iodine atom follows rupture of the Sb–S bond. In the latter, however, the Bi–I and Bi–S bonds are ruptured simultaneously.

Accordingly, for the thermal decomposition of iodo-(piperidyldithiocarbamate) complexes of Sb(III) and Bi(III) we propose the general mechanism shown in Scheme 1.

The studied complexes are monomeric, with the dithiocarbamato groups acting as bidentate ligands, and have a square pyramidal structure with the iodine atom on top [17].

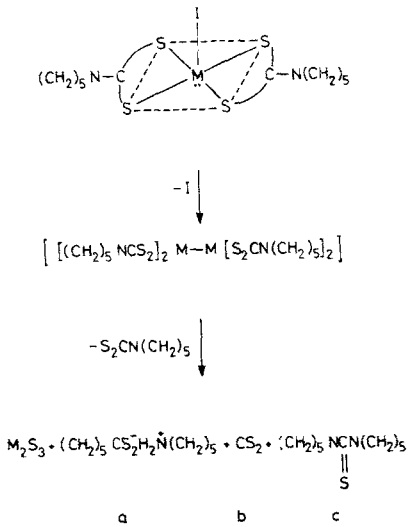

Schemes 1 Thermal decomposition of the complexes $IM[S_2CN(CH_2)_5]_2$ (M = As, Sb, Bi)

The intermediate dimeric product $M_2[S_2CN(CH_2)_5]_4$ was not isolated, the reason probably being its instability at temperatures higher than 250°. It rather decomposes just after its formation to give the final products $M^0 + M_2S_3$ and the volatile compounds *a*, *b* and *c*, in the same manner as reported earlier [6].

The reaction path for the thermal decomposition of the iodo derivatives is in line with the fragmentation pattern in their mass spectra [17]. Study of these spectra reveals the absence of the molecular ion $M^{+\cdot}$, whereas the ionic fragments $M(S_2CNR_2)^{7+\cdot}$ and $I\overset{+}{M}(S_2CNR_2)$ were found; these can be produced by removing either a iodine atom or a dithiocarbamato group from the parent compound. The ionic fragments detected at lower *m/e* values are considered to be products of the pyrolytic decomposition of the initial fragments in the probe by the removal of the species R_2NCS_2, R_2NCS and I. The basic peak could be due either to R_2NCS^{7+} or to $CS_2^{7+\cdot}$, depending on the temperature at which the spectrum was taken. The ions observed at lower *m/e* values were those corresponding to the decomposition of a dithiocarbamato group. In order to complete our study, we took the mass spectra of the complexes $XSb[S_2CN(CH_2)_5]_2$ (X = Br and Cl). The main features of these spectra are the absence of the molecular ions and the presence of peaks corresponding to $X\overset{+}{S}b(S_2CN(CH_2)_5)$ and $Sb(S_2CN(CH_2)_5)^{7+\cdot}$. It is worth emphasizing the absence of $\overset{+}{S}b(S_2CN(CH_2)_5)_2$ both from these spectra and from those of the iodo derivatives, which is further support of our view that these two complexes lose their halogen and one dithiocarbamato group simultaneously. The basic peak of the spectra corresponds

to $CS_2^{7+\cdot}$, while ionic fragments due to pyrolytic decomposition of the initial ions were detected at suitable *m/e* values.

Consequently, during the thermal decomposition of the complexes $XSb[S_2CN(CH_2)_5]_2$ (X = Cl and Br), where the metal and the dithiocarbamato group remain the same, we notice that the removal of one dithiocarbamate ligand is accompanied by the simultaneous loss of chlorine and by a gradual loss of bromine, respectively. The mechanism of their thermal decomposition therefore follows that proposed for the corresponding iodo-piperidyldithiocarbamate complexes. The fragmentation pattern in their mass spectra is in accord with the above mechanism, which means that the existence of certain of the detected ions is due to pyrolytic decomposition.

Interpretation of QIA curves

The weight and temperature curves obtained with the QIA technique for all the studied complexes in air are given in Figs 14 to 27. Analysis of these curves showed that these complexes decompose in two or three stages. This situation is reminiscent of that observed in thermogravimetry curves under non-isothermal conditions in air as reported previously [6, 7].

The kinetic data were analyzed through various kinetic expressions, by plotting suitable functions of $g(a)$ (see theoretical part) *vs* time. k values for the linear region were then calculated from the appropriate equation or from the slope of the corresponding straight line.

For all the studied complexes, the data obtained from the TG curves in the QIA examination, were tested for all the functions of $g(a)$. The results indicated that in no case did the reaction of the first decomposition stage follow a diffusion-controlled mechanism (D) or an Avrami mechanism (A_2, A_3). Instead, it was found that the thermal decomposition obeys n-order reaction kinetics or the power law, where $f(a)$ could be a^n or $(1-a)^n$. The valid values of n are 0, 1/2, 2/3, 1 and 2. The order of reaction (n) is different for each complex.

An example of the evaluation of the kinetic parameters (rate constant k and reaction order n) is given for the complex $Bi[S_2CN(CH_2)_5]_3$. The values obtained are presented in Table 6 and in Figs 28 and 29. We can see that only the $a^{1/3}$ function exhibits a good linear correlation with time. The reaction is therefore controlled by the power law with the order of reaction equal to 2/3. The k value was found to be $(6.26 \pm 0.2) \times 10^{-2}$ min^{-1} with $r^2 = 0.9953$.

The results of kinetic analysis for the studied tris(dithiocarbamates) and halo-bis(dithiocarbamates) are given in Tables 7 and 8, respectively. From these we can see the equation which best describes the decomposition reaction at a certain temperature. The regression coefficient r^2 is also given for each equation, as well as the validity range for the fraction of reactant decomposed (a).

It is obvious that for some complexes the first decomposition stage consists of two parts (a change in slope in the curve) which may or may not be controlled by the

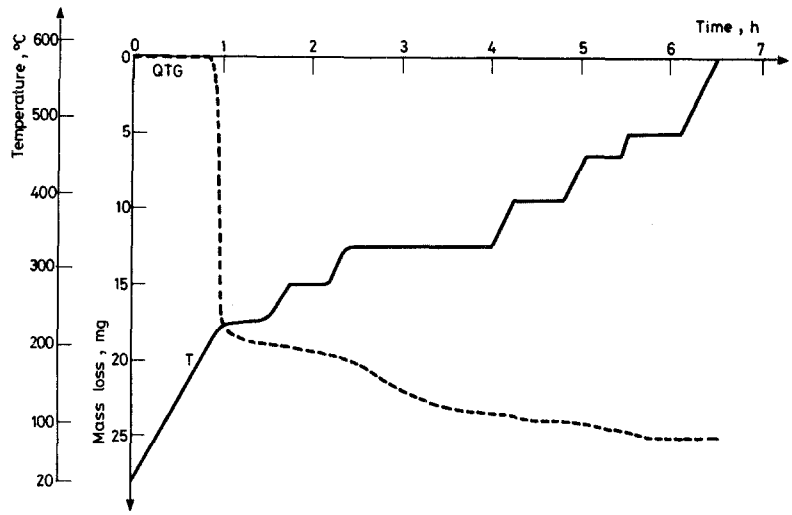

Fig. 14 Weight and temperature curves for $As[S_2CNEt_2]_3$ obtained with the QIA technique in air

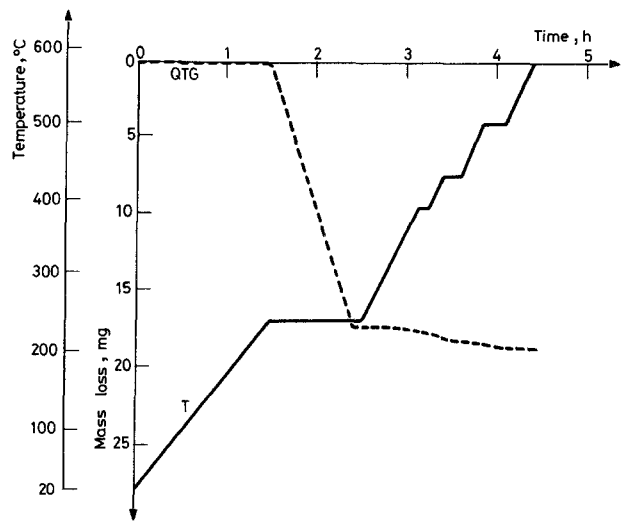

Fig. 15 Weight and temperature curves for $Sb[S_2CNEt_2]_3$ obtained with the QIA technique in air

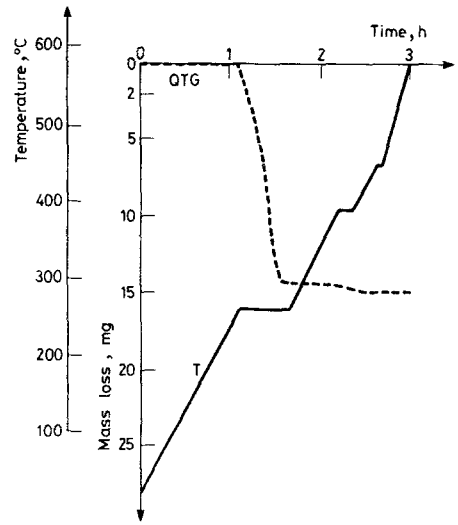

Fig. 16 Weight and temperature curves for $Bi[S_2CNEt_2]_3$ obtained with the QIA technique in air

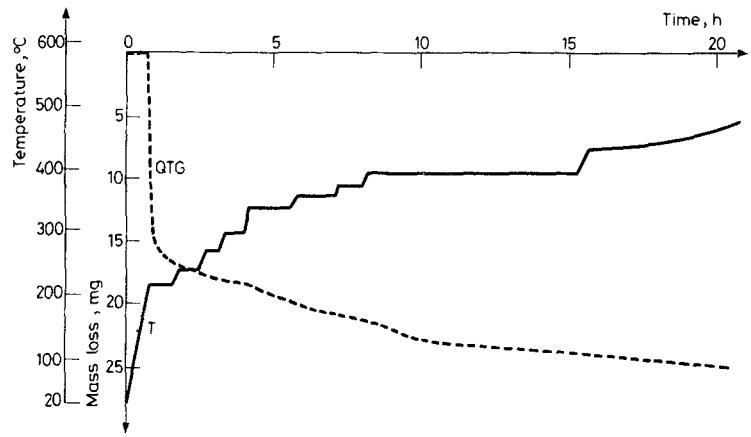

Fig. 17 Weight and temperature curves for $As[S_2CN(CH_2)_5]_3$ obtained with the QIA technique in air

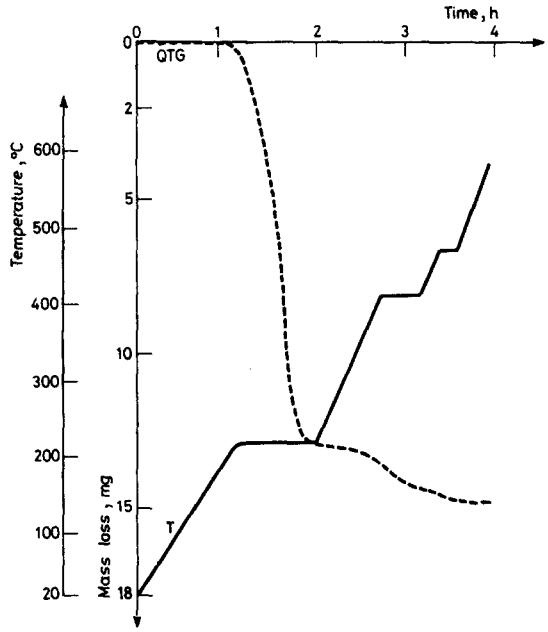

Fig. 18 Weight and temperature curves for $Sb[S_2CN(CH_2)_5]_3$ obtained with the QIA technique

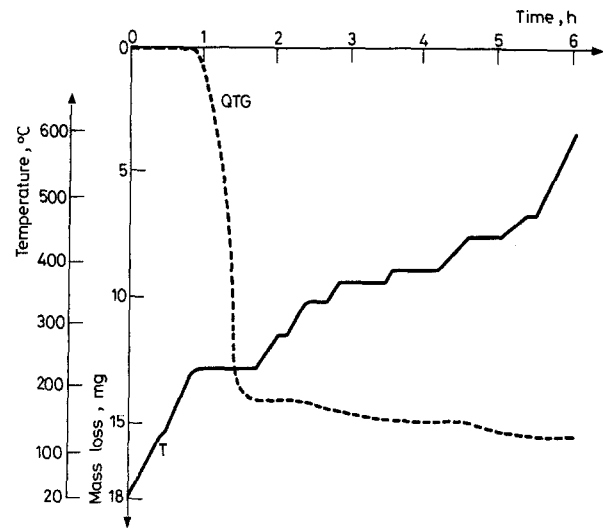

Fig. 19 Weight and temperature curves for $Bi[S_2CN(CH_2)_5]_3$ obtained with the QIA technique in air

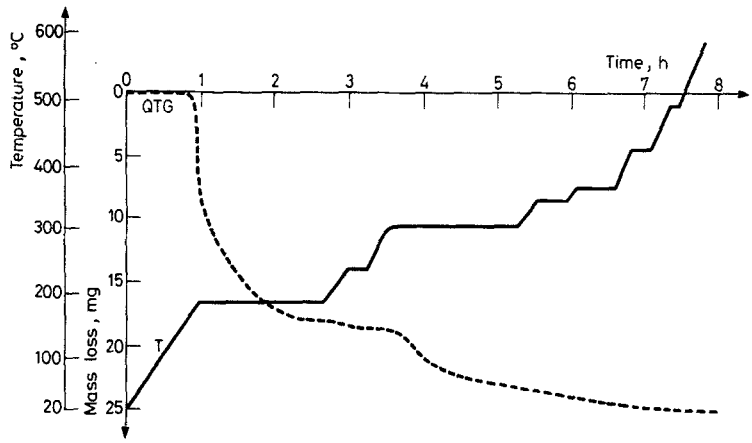

Fig. 20 Weight and temperature curves for $As[S_2CN(CH_2)_4O]_3$ obtained with the QIA technique in air

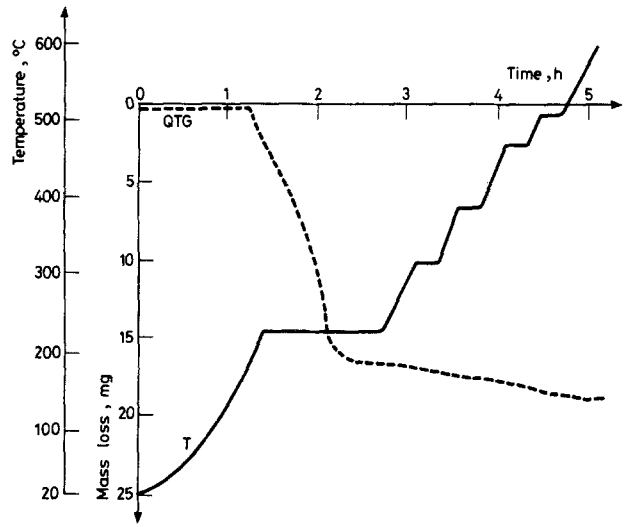

Fig. 21 Weight and temperature curves for $Sb[S_2CN(CH_2)_4O]_3$ obtained with the QIA technique in air

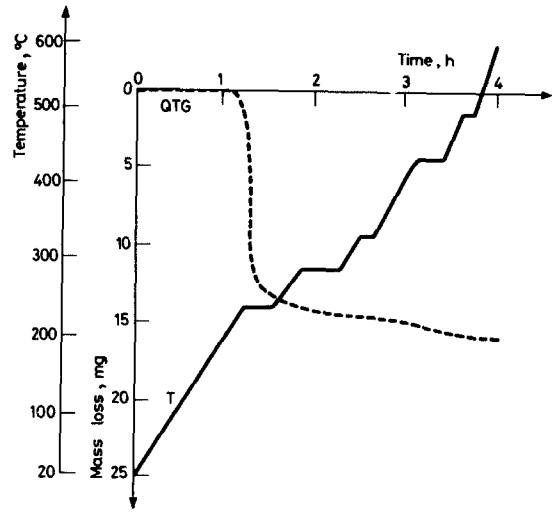

Fig. 22 Weight and temperature curves for $Bi[S_2CN(CH_2)_4O]_3$ obtained with the QIA technique in air

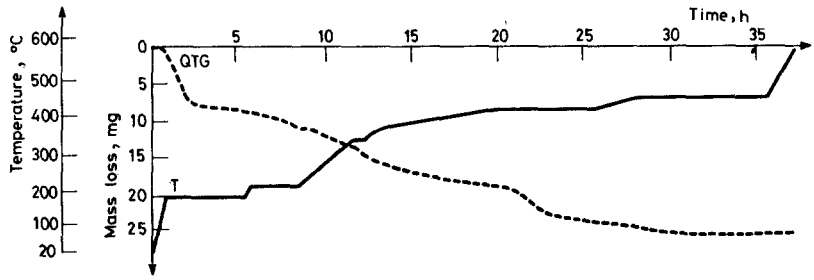

Fig. 23 Weight and temperature curves for $IAs[S_2CN(CH_2)_5]_2$ obtained with the QIA technique in air

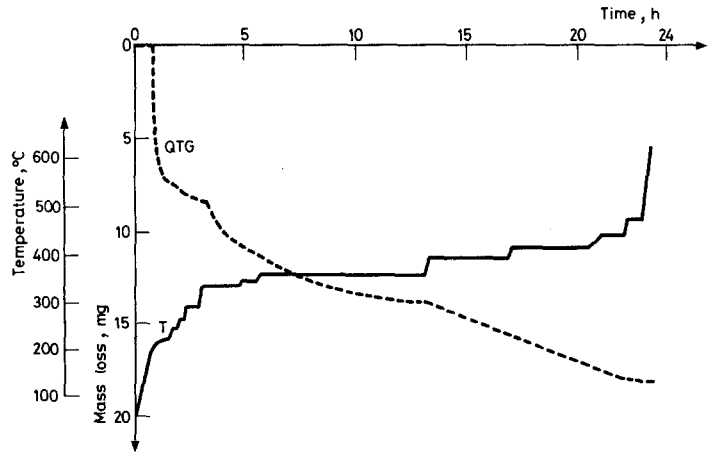

Fig. 24 Weight and temperature curves for $ISb[S_2CN(CH_2)_5]_2$ obtained with the QIA technique in air

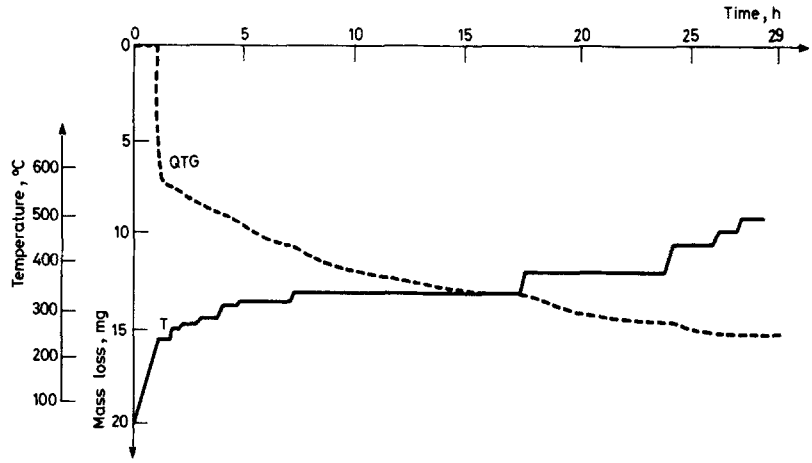

Fig. 25 Weight and temperature curves for $IBi[S_2CN(CH_2)_5]_2$ obtained with the QIA technique in air

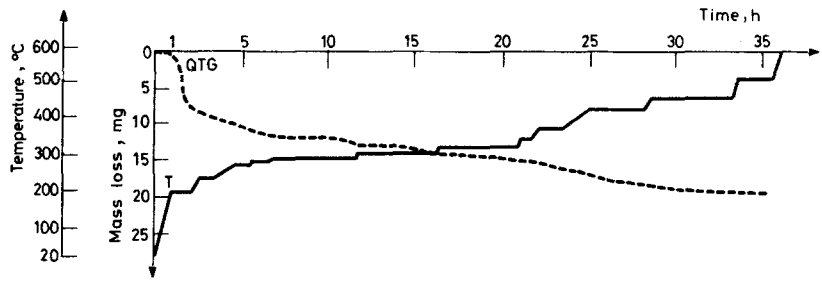

Fig. 26 Weight and temperature curves for $BrSb[S_2CN(CH_2)_5]_2$ obtained with the QIA technique in air

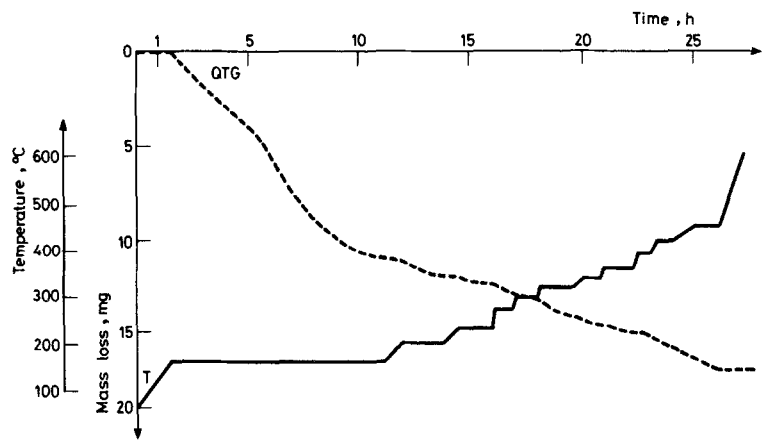

Fig. 27 Weight and temperature curves for $ClSb[S_2CN(CH_2)_5]_2$ obtained with the QIA technique in air

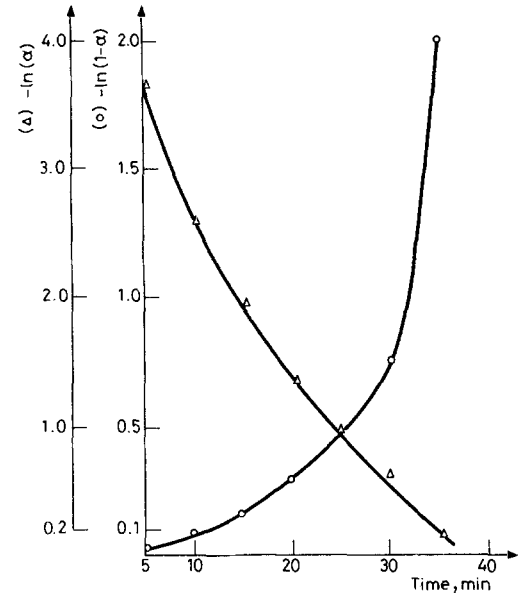

Fig. 28 Plots of $g(a)$ *vs.* time, for first-order reactions controlled from Random Nucleation mechanism or Exponential law. $n = 1$

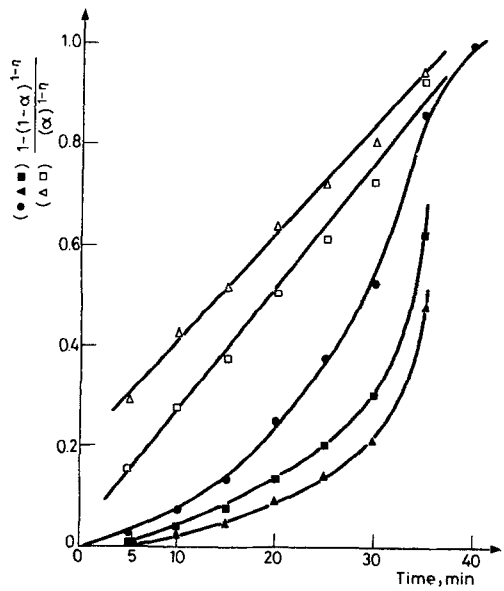

Fig. 29 Plots of $g(a)$ *vs.* time, for "n-order" reactions controlled from different mechanisms according to references [13, 14]. ▲ $n = 2/3$, ■ $n = 1/2$, ● $n = 0$, △ $n = 2/3$, □ $n = 1/2$

Table 6 Numerical data of functions $g(a)$ *vs.* time, for different values of fraction a, assuming various kinetic equations

t, min	w, mg	a	$-\ln a$	$\frac{1}{a}$	$a^{1/2}$	$a^{1/3}$	a^2	$1-a$	$-\ln(1-a)$	$(1-a)^{1/2}$	$1-(1-a)^{1/2}$	$1-(1-a)^{1/3}$
0	0		—	—	—	—	—	1.000	—	—	—	—
5	0.35	0.35	3.649	38.46	0.161	0.296	0.006	0.974	0.026	0.988	0.012	0.008
10	1.07	0.079	2.538	12.66	0.281	0.429	0.0062	0.921	0.082	0.959	0.040	0.027
15	1.95	0.143	1.945	6.99	0.378	0.523	0.0204	0.857	0.154	0.925	0.074	0.050
20	3.55	0.261	1.343	3.83	0.510	0.639	0.0681	0.739	0.302	0.859	0.140	0.095
25	5.17	0.380	0.967	2.63	0.616	0.724	0.1444	0.620	0.478	0.787	0.212	0.147
30	7.20	0.529	0.636	1.89	0.727	0.808	0.2798	0.471	0.753	0.686	0.313	0.222
35	11.75	0.864	0.146	1.16	0.929	0.950	0.7460	0.136	1.995	0.368	0.631	0.485
40	13.60	1.000	—	—	—	—	—	—	—	—	—	—

Table 7 Kinetic results of the first decomposition stage of some tris(dithiocarbamates) by assuming different reactions mechanisms

Complex		Validity range of a	T, °C	Equation which describes the decomposition	n	k, min^{-1}	Mechanism	Symbol*
$As[S_2CNEt_2]_3$		0.12–0.90	220	$\ln a = kt$ **($r^2 = 0.9929$)	1	0.517±0.03	exponential law	–
$Sb[S_2CNEt_2]_3$		0.15–0.94	240	$a = kt$ ($r^2 = 0.9996$)	0	$(1.95\pm0.2) \times 10^{-2}$	zero order mechanism (Polany–Wigner equation)	R_1
$Bi[S_2CNEt_2]_3$		0.06–0.90	260	$3a^{1/3} = kt$ ($r^2 = 0.9978$)	2/3	$(6.62\pm0.18) \times 10^{-2}$	Power law	–
$As[S_2CN(CH_2)_5]_3$	i)	0.00–0.84	210	$-\ln(1-a) = kt$ ($r^2 = 0.9995$)	1	0.284±0.006	First-order mechanism (Random Nucleation)	F_1
	ii)	0.84–0.99	210	$-\ln(1-a) = kt$ ($r^2 = 0.9958$)	1	$(7.5\pm0.2) \times 10^{-2}$	(Random Nucleation)	F_1
$Sb[S_2CN(CH_2)_5]_3$		0.02–0.97	220	$2a^{1/2} = kt$ ($r^2 = 0.9994$)	1/2	$(4.25\pm0.04) \times 10^{-2}$	Power law	–
$Bi[S_2CN(CH_2)_5]_3$		0.02–0.86	227	$3a^{1/3} = kt$ ($r^2 = 0.9953$)	2/3	$(6.26\pm0.2) \times 10^{-2}$	Power law	–
$As[S_2CN(CH_2)_4O]_3$	i)	0.05–0.54	190	$3a^{1/3} = kt$	2/3	0.258	Power law	–
	ii)	0.54–0.99	190	$3[1-(1-a)^{1/3}] = kt$ **($r^2 = 0.9997$)	2/3	$(2.24\pm0.001) \times 10^{-2}$	Two-thirds order mechanism (Phase boundary)	R_3
$Sb[S_2CN(CH_2)_4O]_3$	i)	0.10–0.15	230	$3[1-(1-a)^{1/3}] = kt$	2/3	0.133	Two-thirds order mechanism (Phase boundary)	R_3
	ii)	0.15–0.98	230	$3a^{1/3} = kt$ ($r^2 = 0.9992$)	2/3	$(3.17\pm0.05) \times 10^{-2}$	Power law	–
$Bi[S_2CN(CH_2)_4O]_3$		0.01–0.86	240	$3a^{1/3} = kt$	2/3	$(13.6\pm1.2) \times 10^{-2}$	Power law	–

* The symbols are given from Achar et al. [26]; ** Regression coefficient.

Table 8 Kinetic results of the first decomposition stage of some halo-bis(dithiocarbamates) by assuming different reactions mechanism

Complex		Validity range of a	T, °C	Equation which describes the decomposition	n	k, min^{-1}	Mechanism	Symbol*
$IAs[S_2CN(CH_2)_5]_2$	i)	0.13–0.77	170	$a = kt$ **($r^2 = 0.9999$)	0	$(10.65 \pm 0.01) \times 10^{-3}$	zero order mechanism (Polany–Wigner equation)	R_1
	ii)	0.77–0.99	170	$a = kt$ ($r^2 = 0.9953$)	0	$(6.5 \pm 0.3) \times 10^{-4}$	(Polany–Wigner equation)	R_1
$ISb[S_2CN(CH_2)_5]_2$		0.38–0.98	225	$-\ln(1-a) = kt$ ($r^2 = 0.9991$)	1	$(1.53 \pm 0.6) \times 10^{-1}$	First-order mechanism (Random Nucleation)	F_1
$IBi[S_2CN(CH_2)_5]_2$		0.38–0.98	240	$-\ln(1-a) = kt$ ($r^2 = 0.9939$)	1	$(18.16 \pm 0.6) \times 10^{-2}$	(Random Nucleation)	F_1
$BrSb[S_2CN(CH_2)_5]_2$	i)	0.06–0.84	195	$\ln \frac{a}{1-a} = kt$ ($r^2 = 0.9930$)	–	0.138 ± 0.008	Prout–Tompkins equation	–
	ii)	0.84–0.99	195	$-\ln(1-a) = kt$ ($r^2 = 0.9980$)	1	0.128 ± 0.35	Random Nucleation	F_1
$ClSb[S_2CN(CH_2)_5]_2$	i)	0.06–0.46	160	$a = kt$ ($r^2 = 0.9997$)	0	$(1.72 \pm 0.01) \times 10^{-3}$	zero order mechanism (Polany–Wigner equation)	R_1
	ii)	0.46–0.99	160	$3[1-(1-a)^{1/3}] = kt$ ($r^2 = 0.9975$)	2/3	$(5.70 \pm 0.06) \times 10^{-3}$	Two-thirds order mechanism (Phase boundary)	R_3

* The symbols are given from Achar et al. [26]; ** Regression coefficient.

same mechanism. For complexes with the same metals, the decomposition is described by similar equations, while the values of the rate constants (k, min^{-1}) have the same order of magnitude. Thus, we can conclude that the nature of the metal influences the decomposition mechanism of these dithiocarbamate complexes. The k values are within the limits referred to in the literature for the thermal decomposition of solid complexes or salts of various metals [24, 25].

References

1 G. D'Ascenzo, V. Carunchio and A. Messina, Thermochim. Acta, 2 (3) (1971) 211.
2 G. K. Bratspies, J. F. Smith, J. O. Hill and R. J. Magee, Thermochim. Acta, 19 (1977) 335.
3 G. K. Bratspies, J. F. Smith and J. O. Hill, Thermochim. Acta, 19 (1977) 373.
4 N. K. Kaushik, G. R. Chhatwal and A. K. Sharma, Thermochim. Acta, 58 (1982) 231.
5 G. D'Ascenzo and T. Bica, Thermochim. Acta, 18 (1977) 301.
6 M. Lalia-Kantouri, A. Christofides and G. E. Manoussakis, J. Thermal Anal., in press.
7 M. Lalia-Kantouri and G. E. Manoussakis, J. Thermal Anal., submitted for publication.
8 J. Paulik and F. Paulik, Hungarian Scientific Instruments, 34 (1975).
9 J. Paulik, F. Paulik, E. Buzágh-Gere and M. Arnold, Thermochim. Acta, 31 (1979) 93.
10 J. Rouquerol, J. Thermal Anal., 5 (1973) 203.
11 O. Toft Sørensen, Thermochim. Acta, 29 (1979) 211.
12 V. Swaminathan and N. S. Madhavan, J. Anal. Appl. Pyrolysis, 3 (2) (1981) 131.
13 J. M. Criado and J. Morales, Thermochim. Acta, 19 (1977) 305.
14 J. M. Criado, J. Morales and V. Rives, J. Thermal Anal. 14 (1978) 221.
15 G. E. Manoussakis and C. A. Tsipis, J. Inorg. Nucl. Chem., 35 (1973) 743.
16 R. G. Luchtefeld, Res. Tech. Rep., 1 (1976) 19–73 (Chem. Abs., 88 (14) (1978) 98614 t).
17 C. A. Tsipis and G. E. Manoussakis, Inorg. Chim. Acta, 18 (1976) 35.
18 C. L. Raston and A. H. White, J. C. S. Dalton, 3 (1975) 2425.
19 C. L. Raston and A. H. White, J. C. S. Dalton, 9 (1976) 791.
20 L. Reich and D. W. Levi, Makromolek. Chem. 66 (1963) 102.
21 G. O. Doak and L. D. Freeman, Organometallic Compounds of Arsenic, Antimony and Bismuth, John Wiley, 1970, p. 11.
22 E. S. Freeman and B. Carroll, J. Phys. Chem., 62 (1958) 394.
23 G. O. Piloyan, I. D. Ryabchnikov and O. S. Novikova, Nature, 212 (1966) 1229.
24 S. K. Dhar and Basolo, J. Inorg. Nucl. Chem., 25 (1963) 37.
25 T. Palanisamy, J. Gopalakrishnan, B. Viswanathan, V. Srinivasan and M. V. C. Sastri, Thermochim. Acta, 2 (1971) 265.
26 B. N. Achar, G. W. Brindley and J. H. Sharp, Proc. Intern. Clay Conf., Jerusalem, 1 (1966).

Zusammenfassung — Einige helo-Dithiocarbamate der allgemeinen Formal $XM[S_2CN(CH_2)_5]_2$ (X = Cl, Br und I; M = As, Sb und Bi) wurden mittels simultaner TG/DTG/DTA unter nichtisothermen Bedingungen in Luft und Stickstoff untersucht. Für den ersten Zersetzungsschritt wurden E^*-Werte durch graphische Methoden bestimmt und die TIN-Temperaturen aus den TG-Profilen berechnet. Ein auf den Ergebnissen der Thermogravimetrie und Pyrolyse sowie auf massenspektroskopischen Daten beruhender möglicher Mechanismus wird vorgeschlagen. Fünf der angeführten Dithiocarbamate und 9 Komplexe der allgemeinen Formel $M[S_2CN<]_3$ (M = As, Sb und

Bi; $N = NEt_2$, $N(CH_2)_5$ und $N(CH_2)_4O$) wurden mittels QIA (quasi-isotherme Analyse) in Luft untersucht. Als Beispiel ist die Bestimmung der kinetischen Parameter (k und n) für den ersten Schritt der Zersetzung von $Bi[S_2CN(CH_2)_5]_3$ unter Annahme verschiedener kinetischer Gleichungen angegeben.

Резюме — Совмещенным методом ТГ, ДТГ и ДТА в неизотермических условиях в атмосфере воздуха и азота изучены комплексы галоген-дитиокарбаматов с общей формулой $XM[S_2CN(CH_2)_5]_2$, где X = Cl, Br и I, а M = As, Sb и Bi. Значения E^* для первой стадии разложения были вычислены графическими методами, а ТИН температуы были определены из профилей ТГ-кривых. На основе полученных результатов и данных масс-спектров предложен возможный механизм реакции разложения. Методом квазиизотермического анализа в атмосфере воздуха проведен анализ кинетики реакции разложения пяти вышеупомянутых дитиокарбаматных комплексов и девяти комплексов с общей формулой $M[S_2CN<]_3$, где M = As, Sb и Bi, а $N< = NEt_2$, $N(CH_2)_5$ и $N(CH_2)_4O$. На основе различных кинетических уравнений определены параметры k и n первой стадии разложения комплекса $Bi[S_2CN(CH_2)_5]_3$.